

# Measurements of $^{115}\text{In}(\gamma, n)$ reaction cross-sections using bremsstrahlung photon irradiation

T. Krasta<sup>1</sup>, A. Chekhovska<sup>2</sup>, D. Chvátíl<sup>3</sup>, I. Krausova<sup>3</sup>, V. Olšanský<sup>3</sup>, D. Riekstiņa<sup>1</sup>

<sup>1</sup> Institute of Solid State Physics, University of Latvia

<sup>2</sup> National Science Center “Kharkiv Institute of Physics and Technology”

<sup>3</sup> Nuclear Physics Institute of the Czech Academy of Sciences



INSTITUTE OF SOLID STATE PHYSICS  
UNIVERSITY OF LATVIA

## Introduction:

Nuclear region with  $100 < A < 130$  is an important playground for the study of cosmic nucleosynthesis of elements heavier than iron when reactions become endoenergetic. Such nucleosynthesis is governed by a complex interplay between capture reactions and radioactive decay [1]. Study of the origin and abundances of elements requires experimental data about various nuclear reactions (Fig.1). The knowledge about photo nuclear reaction cross sections is especially important.

Characteristic feature of Cd ( $Z=48$ ), In ( $Z=49$ ), Sn ( $Z=50$ ), and Sb ( $Z=51$ ) nuclei (Fig.2) is a high number of isomer states which serve as important waiting points in the nucleosynthesis processes. It is explained by the pronounced nuclear shell effects and nuclear shape coexistence in the vicinity of proton magic number  $Z=50$  and neutron magic number  $N=82$ .

Photonuclear reactions of indium isotopes attract nowadays considerable attention due to their importance for nucleosynthesis processes of proton-rich p-nuclei, such as  $^{114}\text{Sn}$ , and  $^{113}\text{In}$ .

## Methods:

The experiment to study the natural In target (95.7%  $^{115}\text{In}$  and 4.3%  $^{113}\text{In}$ ) was conducted using bremsstrahlung photon radiation from the Microtron MT-25 [2] of the Nuclear Physics Institute, Czech Academy of Sciences (Prague). The experimental set-up scheme is shown on Fig 3. Gold (Au) and copper (Cu) foils were used as monitor targets. Irradiation was carried out at the end point bremsstrahlung energies  $E_{\gamma, \text{max}} = 7.17, 8.11, 9.75, 12.12, 13.79, 16.6, 18.34, 20.36, \text{ and } 22.82 \text{ MeV}$ .

The decay  $\gamma$ -spectra from irradiated targets were measured using a spectrometer based on a HPGe detector with efficiency = 30% and resolution = 1.8 keV for 1332 keV  $\gamma$ -line of  $^{60}\text{Co}$ .

Fig. 4 and 5 present the schemes of nuclear decay of  $^{113}\text{In}$  and  $^{115}\text{In}$ , leading to the formation of  $^{112}\text{Cd}$  or  $^{112}\text{Sn}$  and  $^{114}\text{Cd}$  or  $^{114}\text{Sn}$ , respectively (The data taken from NuDat3). Vertical arrows correspond to radiative transitions between energy levels of decaying radioactive nuclei. Energy of  $\gamma$ -transitions in keV and corresponding intensity in % are indicated next to vertical arrows.

## Results:

Fig.7 shows obtained experimental photoactivation cross-sections (black squares): a) of the  $^{115}\text{In}(\gamma, \gamma')^{115\text{m}}\text{In}$  reaction; b) of the  $^{115}\text{In}(\gamma, n)^{114\text{m}}\text{In}$  reaction; and c) of the  $^{115}\text{In}(\gamma, n)^{114\text{g}}\text{In}$  reaction.

The curves on graphs present the results of TALYS computer code [3] calculations in the frameworks of statistical theory using different combinations of nuclear levels density and radiation strength function parameters.

The cross-sections of  $^{115}\text{In}(\gamma, \gamma')^{115\text{m}}\text{In}$  reaction show good agreement with the results of TALYS calculations using the back-shifted Fermi gas model for nuclear level density and the Brink-Axel Lorentzian for the radiation strength function (blue curve).

The experimental cross-sections of  $^{115}\text{In}(\gamma, n)^{114\text{m}}\text{In}$  reaction show good agreement with the results of TALYS calculations with the back-shifted Fermi-gas model for nuclear level density and Kopecky-Uhl generalized Lorentzian for radiation strength function (red curve), while the  $^{115}\text{In}(\gamma, n)^{114\text{g}}\text{In}$  reaction cross-sections are better described with the constant temperature+Fermi-gas model for nuclear level density and Kopecky-Uhl generalized Lorentzian for  $\gamma$ -function (black curve).

## Conclusions:

1. Cross-sections for the  $^{115}\text{In}(\gamma, \gamma')^{115\text{m}}\text{In}$ ,  $^{115}\text{In}(\gamma, n)^{114\text{m}}\text{In}$  and  $^{115}\text{In}(\gamma, n)^{114\text{g}}\text{In}$  reactions at bremsstrahlung photon end point energies 8.11, 9.75, 12.12, 13.79, 16.6, 18.34, 20.36 and 22.82 MeV were determined.
2. Obtained experimental cross-sections of  $^{115}\text{In}(\gamma, n)^{114\text{m}}\text{In}$  and  $^{115}\text{In}(\gamma, n)^{114\text{g}}\text{In}$  reactions show good agreement with the results of statistical Hauser-Feshbach model calculations using back-shifted Fermi-gas model or constant temperature+Fermi-gas model for nuclear level density and Kopecky-Uhl generalized Lorentzian for radiation strength function.
3. Experimental cross-sections of the  $^{115}\text{In}(\gamma, \gamma')^{115\text{m}}\text{In}$  favour back-shifted Fermi gas model for nuclear level density and the Brink-Axel Lorentzian for the radiation strength function.

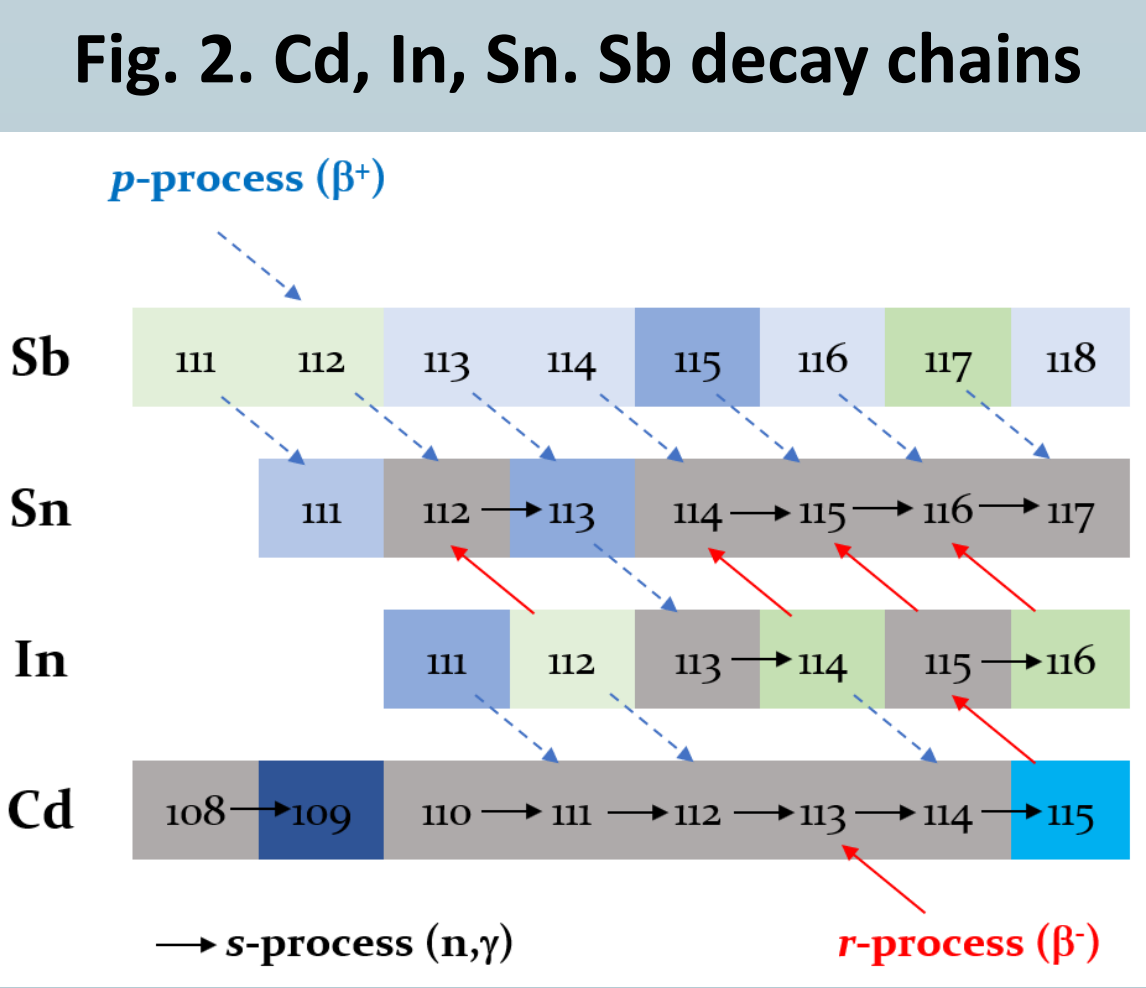
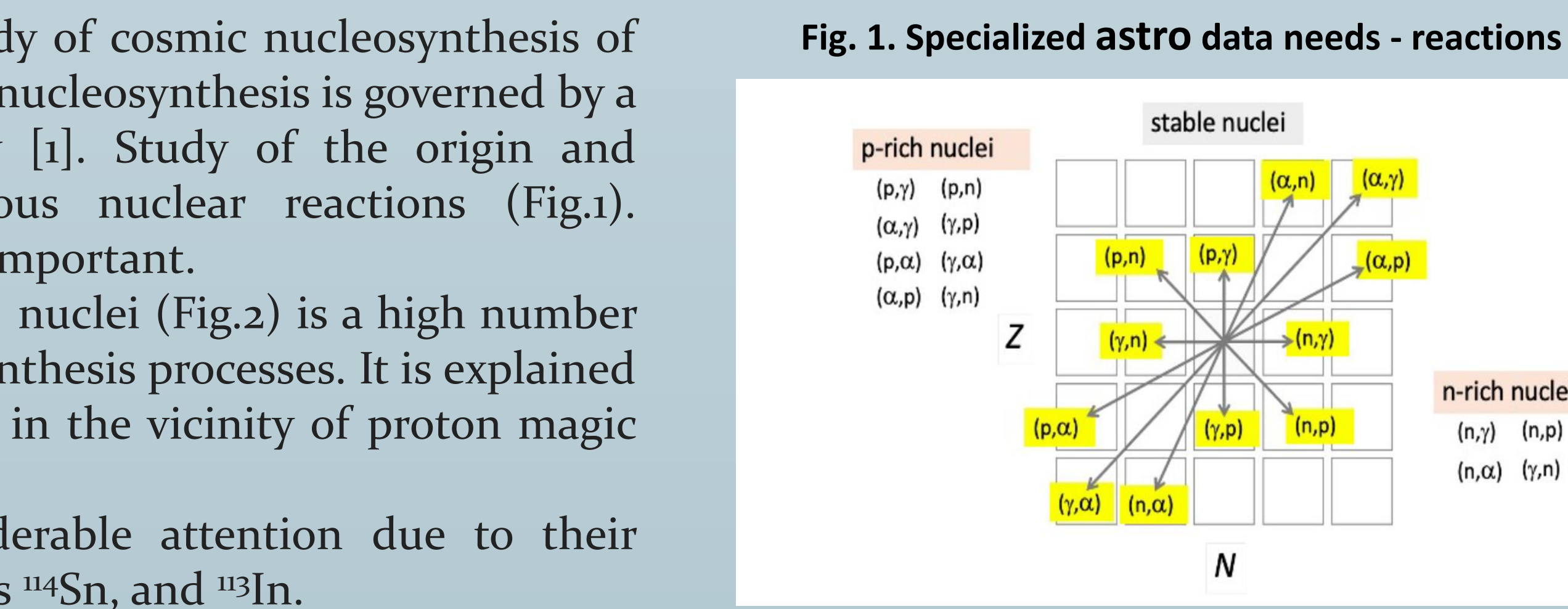
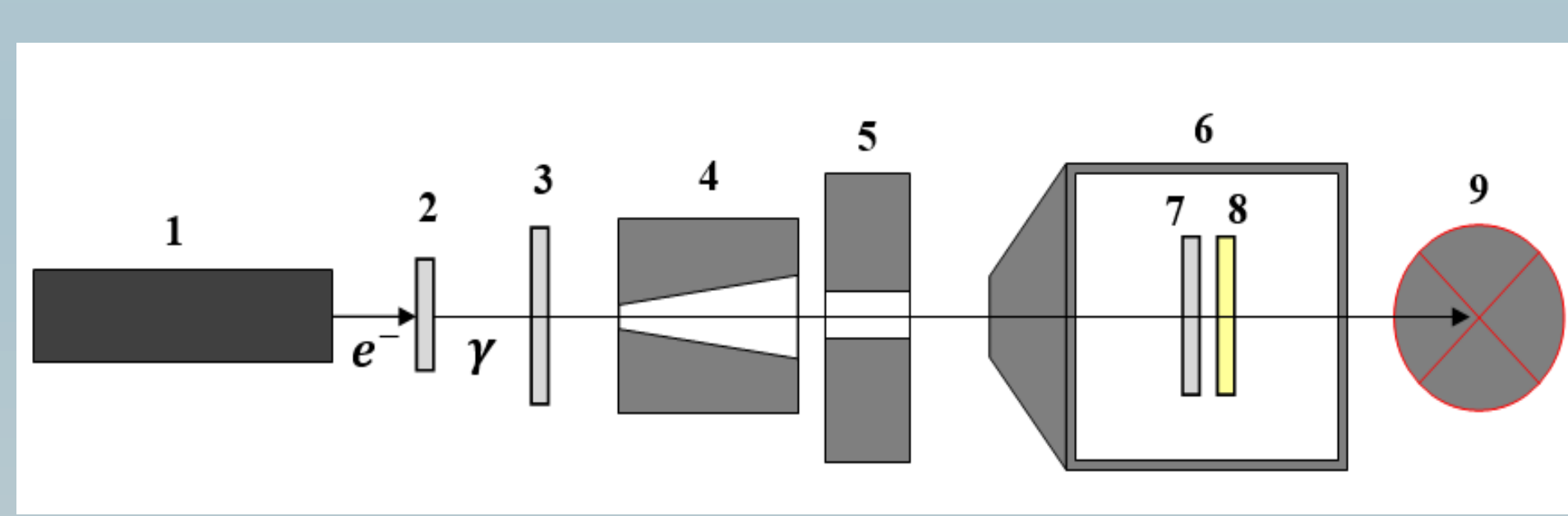


Fig. 3. Experimental set-up



1. Microtron, 2. Converter (with two W targets 1.5 and 3 mm and one Sn foil 0.2 mm), 3. Target with combined Al-Cu scattering foils, 4. Primary conical stainless steel collimator, 5. Secondary square W-steel collimator, 6. Water-cooled chamber, 7. Research target, 8. Monitor target (Cu or Au), 9. Absorber.

Fig. 4. The simplified decay scheme of  $^{113}\text{In}$

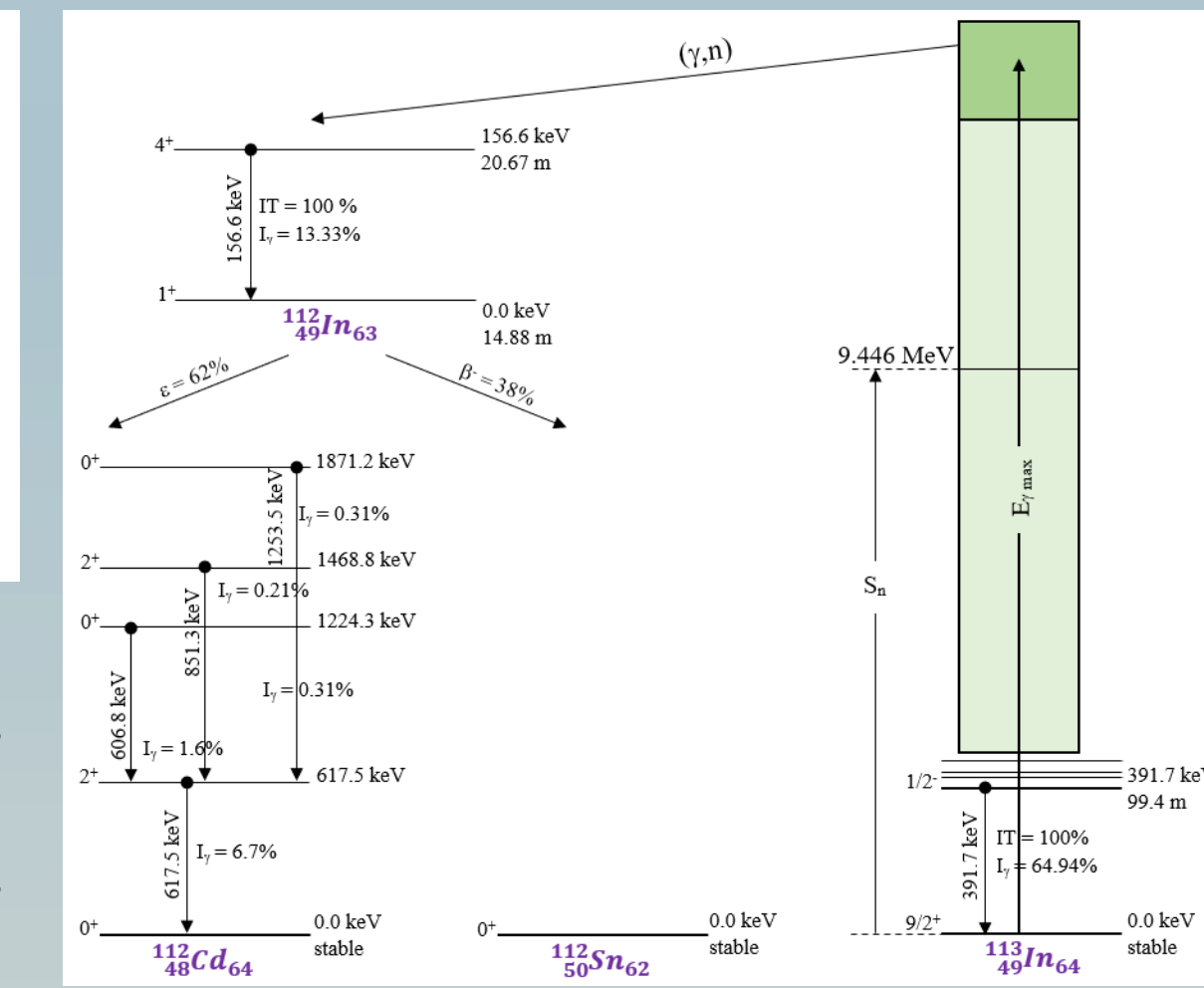


Fig. 5. The simplified decay scheme of  $^{115}\text{In}$

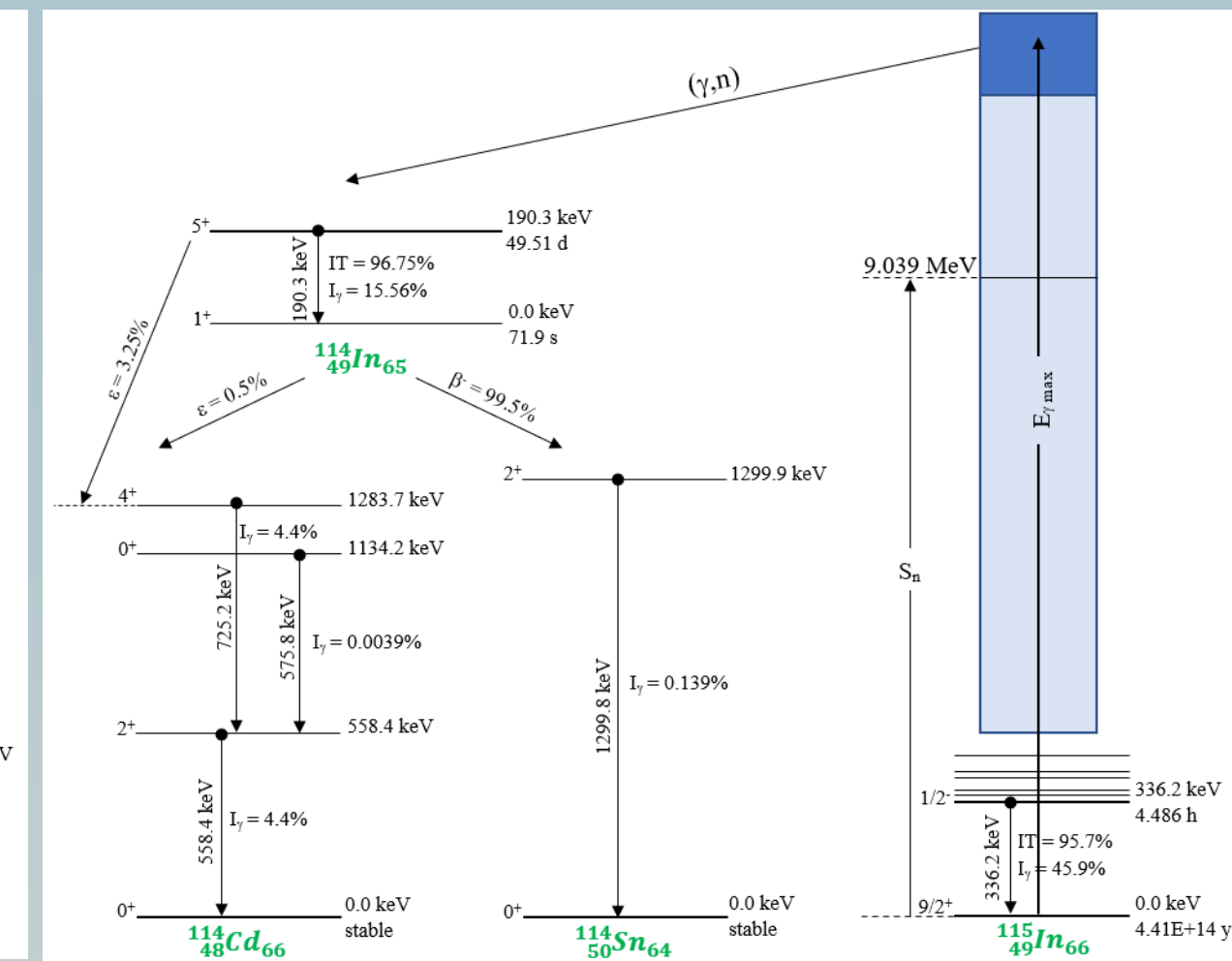


Fig. 6 shows samples of measured decay  $\gamma$ -spectra from activated natural indium target at different irradiation energies ( $E_{\text{irr}}$ ), irradiation times ( $t_{\text{irr}}$ ), cooling times ( $t_{\text{cool}}$ ), measurement times ( $t_{\text{meas}}$ ) and distances from the target to the detector crystal (Dist). Each gamma peak is well identified and assigned to specific nuclei in the decay level schemes of  $^{113}\text{In}(\gamma, \gamma')^{113\text{m}}\text{In}$ ,  $^{113}\text{In}(\gamma, n)^{112\text{g}}\text{In}$ ,  $^{115}\text{In}(\gamma, \gamma')^{115\text{m}}\text{In}$ ,  $^{115}\text{In}(\gamma, n)^{114\text{g}}\text{In}$  reaction products.

Fig. 6. Energy spectra from the activated In target

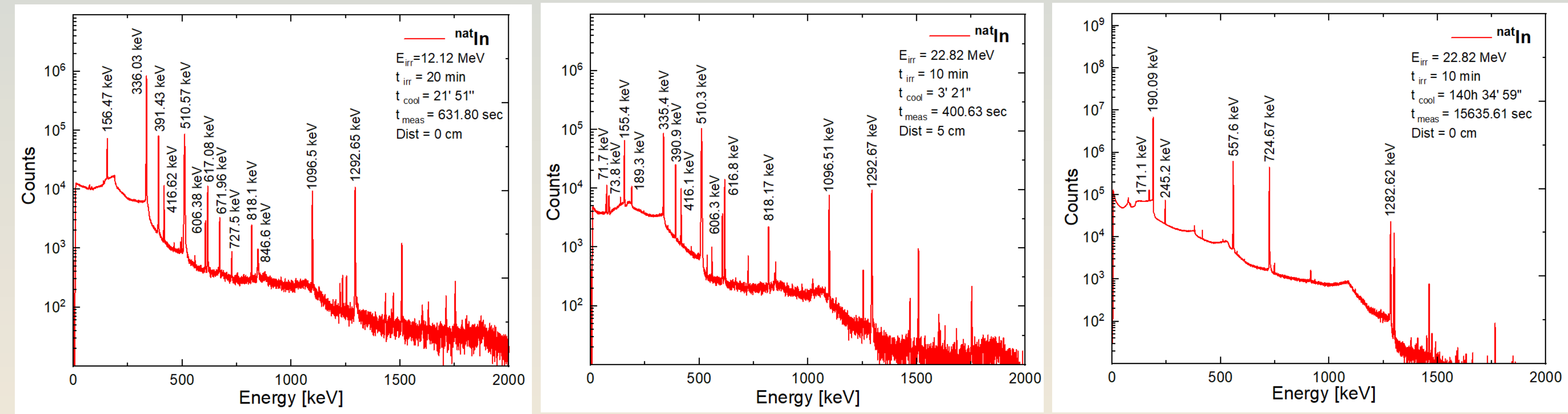
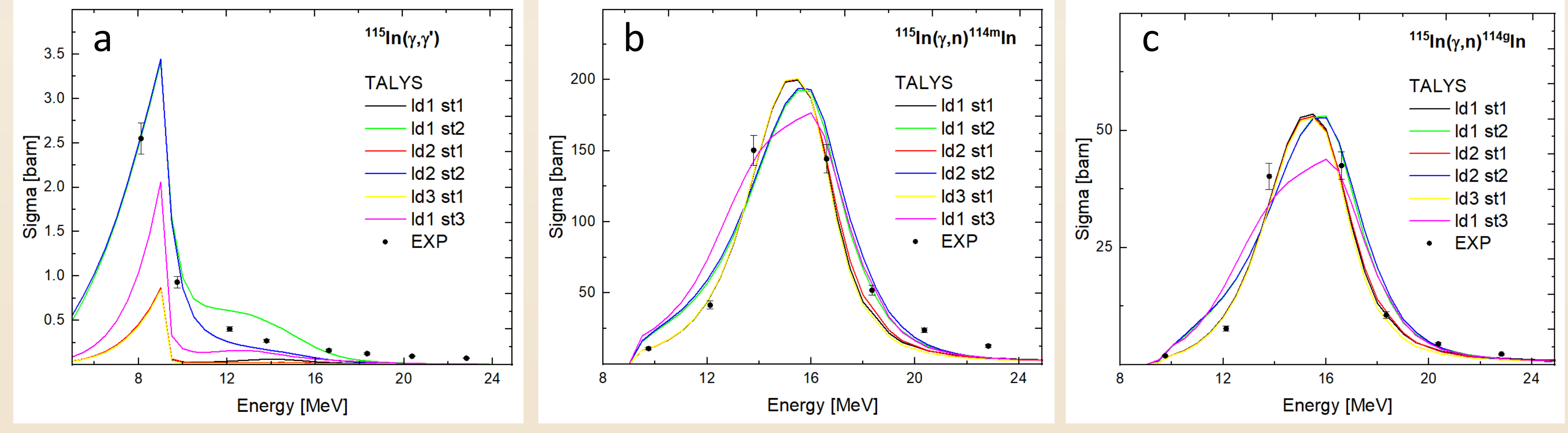


Fig. 7. Cross-sections of  $^{115}\text{In}(\gamma, \gamma')$ ,  $^{115}\text{In}(\gamma, n)^{114\text{m}}\text{In}$  reactions



## References:

1. E. M. Burbidge, G. R. Burbidge, W. A. Fowler and F. Hoyle. Rev. Mod. Phys. v.29, p. 547-650 (1957).
2. P. Krist and J. Bila. Journal of Instrumentation v. 6, T10005 (2011).
3. A. J. Koning and D. Rochman, Nuclear Data Sheets 113, 2841 (2012).

## Contact information:

Anastasiia Chekhovska  
Junior researcher, Institute of High-Energy Physics and Nuclear Physics, National Science Center “Kharkiv Institute of Physics and Technology”  
[chekhovska@kipt.kharkov.ua](mailto:chekhovska@kipt.kharkov.ua)